Infotaxis in practice

Hesselberth, M.

Award date:
2013

Infotaxis in practice

Mark Hesselberth

R-1827-S

August 2013

Abstract

Organisms trying to find nutrients are often faced with the problem of finding the source of an odour in air or water. At macroscopic scales these odours are often spread out over a large area, so that detectable levels are only found highly sporadically. Strategies like chemotaxis, that use chemical concentration gradients to gain information on the location of the odour source, are not applicable in these situations. A macroscopic searcher will therefore need a strategy to locate the source of an odour based on infrequent cues and approximations of the surrounding conditions. One such algorithm is called 'infotaxis', a strategy surrounding the idea of choosing a direction of movement based on the maximum expected gain in information.

The strategy of infotaxis is implemented for two different odour spreading models. One of these applies a mean wind and a time-modulated vortex to apply chaotic advection to the odour particles, the other uses kinematic simulation to replicate the effects of a turbulent flow added to a mean wind. The model of chaotic advection is shown to be effective at diffusing the odour plume from a point source over a certain (near constant) width, and the effectiveness of infotaxis is investigated. The infotaxis algorithm is also applied to the kinematic simulation model and the results are compared to the data gathered in the model of chaotic advection. Analysis of movement based on infotaxis shows large sweeping motions and high density zigzagging.

The strategy of infotaxis shows similarities to movements patterns observed in animals. The idea of a search strategy based on expected gain in information can be applied broadly, for example in algorithms designed for olfactory robots.

Table of contents

1. Introduction

An animal trying to find nutrients is often faced with the problem of finding the source of an odour in air or water. A search strategy like chemotaxis, employed by microscopic organisms, uses chemical concentration gradients to gain information on what direction of travel has the highest chance of getting the animal closer to the source of the odour. However, at macroscopic scales traces of these odours are sometimes separated by large areas where the odour concentration is either zero or at an undetectably low level. Following a gradient will not be possible in these situations. The organism will only be able to detect isolated events where the odour concentration exceeds some detectable level. A macroscopic searcher will therefore need a strategy to locate the source of an odour based on infrequent cues and approximations of the surrounding conditions.

One such algorithm is called 'infotaxis', a strategy surrounding the idea of choosing a direction of movement based on the maximum expected gain in information [1]. When using infotaxis, the aforementioned approximations include assumptions about the rate at which the source is generating the odour and the lifetime of the chemicals that make up the odour. Furthermore, the searcher might be able to estimate the form of the flow in which the search takes place. These approximations can then be used to increase the amount of information gained from the detection of an odour trace.

Movement based on infotaxis shows large sweeping motions and high density zigzagging. These patterns show similarities to those observed in nature, for example in the movements of moths [2]. Infotaxis can be applied in a broad spectrum of fields. An olfactory robot can be used to perform a task similar to the organism mentioned at the start of this text [3]. Similar to that organism, a robot cannot utilize an alternative strategy like chemotaxis when strong chemical concentration gradients are not available. Infotaxis will be a possible solution in that case. This is one application which closely resembles the original inspiration for the strategy, but the general idea of a search strategy based on the expected gain in information can also be applied in more abstract situations involving searching based on sparse information.

In this investigation, the strategy of infotaxis will be implemented for two different odour spreading models. One of these will apply a mean wind and a time-modulated vortex to mix and spread the odour particles, the other will use kinematic simulation to replicate the effects of a turbulent flow added to a mean wind. First, the theory of infotaxis will be given in detail in chapter 2. Then, the methods of applying infotaxis and the implementation of the odour spreading models will be described in chapter 3. In chapter 4, the characteristics of movement based on infotaxis will be evaluated alongside the effectiveness of infotaxis in these situations. Chapter 5 will contain the conclusions drawn from the previous results, as well as recommendations and ideas for further investigation.

2. Theory of infotaxis

2.1 Introduction

In this investigation the search algorithm used is called 'infotaxis'. This strategy is designed to work under conditions where only sporadic cues are available. Almost exclusively low concentrations of the chemical that forms the signal (the 'odour') will be present, with small areas of higher concentration. While a strategy such as chemotaxis is designed to choose a path based on increasing concentration of the odour, such a strategy will not be effective when there is no strong gradient to be measured, only small patches of high concentration and large areas with no detectable signal. In this situation, infotaxis attempts to locally increase the expected rate of information gain based on the detection of these patches. [1]

2.2 Rate of odour encounters in the turbulent medium

To obtain a statistical description of the rate of odour encounters ('hits'), a model is considered where detectable 'particles' are emitted by a source point. These particles are emitted at a rate R, have a finite lifetime τ, propogate with isotropic effective diffusivity D and are advected by a mean wind V. With a source located at position $\vec{r}_0$, the mean stationary concentration field $c(\vec{r}|\vec{r}_0)$ at position $\vec{r}$ will satisfy the advection-diffusion equation

$$0 = -V\,\nabla_y\, c(\vec{r}|\vec{r}_0) + D\Delta c(\vec{r}|\vec{r}_0) - \frac{1}{\tau}c(\vec{r}|\vec{r}_0) + R\delta(\vec{r}-\vec{r}_0) \tag{1}$$

where the wind has been taken to blow in the positive y-direction. In 2D, the solution to this equation is [1]

$$c(\vec{r}|\vec{r}_0) = \frac{R}{2\pi D} e^{\frac{(y-y_0)V}{2D}} K_0\left(\frac{|\vec{r}-\vec{r}_0|}{\lambda}\right); \qquad \lambda = \sqrt{\frac{D\tau}{1+\frac{V^2\tau}{4D}}} \tag{2}$$

where K_0 is the modified Bessel function of order zero. Here, the lifetime τ of particles is considered infinite, so $\lambda \approx \frac{2D}{V}$.

A two-dimensional circular object with diameter a moving through the medium where this source is active will experience a series of encounters at rate $R(\vec{r}|\vec{r}_0)$. In 3D, this rate would be given by [4]

$$R(\vec{r}|\vec{r}_0) = 4\pi\, D\, a\, c(\vec{r}|\vec{r}_0). \tag{3}$$

In 2D, the rate of encounters has a logarithmic divergence and takes the form [1]

$$R(\vec{r}|\vec{r}_0) = \frac{2\pi D c(\vec{r}|\vec{r}_0)}{\ln\left(\frac{\lambda}{a}\right)} = \frac{R}{\ln\left(\frac{\lambda}{a}\right)} e^{\frac{(y-y_0)V}{2D}} K_0\left(\frac{|\vec{r}-\vec{r}_0|}{\lambda}\right). \tag{4}$$

2.3 Probability distribution and reduction of entropy

As mentioned before, infotaxis is a strategy that decides on a path on the basis of increasing the expected rate of information gain. This information is contained in the posterior probability distribution $P_t(\vec{r}_0)$ for the unknown location of the source $\vec{r}_0$. The subscript t represents the fact that the distribution is dynamic, and will be modified during a search.

The probability distribution posterior to experiencing a trace $\mathcal{T}_t$ of uncorrelated odour encounters separated by time intervals V_i without encounters is given by [1]

$$P_t(\vec{r}_0) = \frac{\mathcal{L}_{\vec{r}_0}(\mathcal{T}_t)}{\int \mathcal{L}_{\vec{x}}(\mathcal{T}_t) d\vec{x}} = \frac{\exp\left[-\sum_i \int_{V_i} R(\vec{r}(t')|\vec{r}_0) dt'\right] \prod_{i=1}^{H} R(\vec{r}(t_i)|\vec{r}_0)}{\int \exp\left[-\sum_i \int_{V_i} R(\vec{r}(t')|\vec{x}) dt'\right] \prod_{i=1}^{H} R(\vec{r}(t_i)|\vec{x}) d\vec{x}} \tag{5}$$

where H is the number of hits along the trajectory, t_i are the corresponding times and $\mathcal{L}_{\vec{r}_0}(\mathcal{T}_t)$ is the likelihood of observing the trace $\mathcal{T}_t$ for a source at position $\vec{r}_0$. The absence of correlations allows the distribution to be updated without storing the entire history. The probability distribution after a period δt in which η hits were detected can be calculated from the previous distribution with [5]

$$P_{t+\delta t}(\vec{r}_0) = P_t(\vec{r}_0)\, R^{\eta}(\vec{r}(t+\delta t)|\vec{r}_0)\, e^{-R(\vec{r}(t+\delta t)|\vec{r}_0)\delta t} / Z_{t+\delta t}\,, \tag{6}$$

where $Z_{t+\delta t}$ is a normalizing constant.

In order to obtain a method to quantify the rate of information gain, we consider Shannon's entropy for the distribution [6]

$$S \equiv -\int d\vec{x}\, P(\vec{x}) \ln P(\vec{x}). \tag{7}$$

The entropy shows how uncertain the location of the source is. When the source is located with certainty, the entropy will go to zero. Therefore, the reduction of entropy will quantify the increase in information.

Now, the challenge is to balance the concepts of 'exploration' and 'exploitation'. Here, 'exploitation' would mean moving to locations where $P_t(\vec{r}_0)$ is maximized. Relying purely on this strategy is risky, since the lack of complete information can mean that the searcher will be led far off the track. A safer approach is 'exploration', where gaining more information is preferred over moving. This means either waiting for new information without moving, which is safe but not productive, or searching around a nearby area before moving on to the next.

Infotaxis balances exploration and exploitation by choosing the direction that locally maximizes the expected rate of information acquisition. In order to achieve this, the searcher decides to move to a neighbouring lattice point or standing still, depending on which move maximizes the expected reduction in entropy of the posterior probability field. Consider a searcher at position $\vec{r}$ at time t. The expected reduction in entropy upon moving to neighbouring lattice point $\vec{r}_j$ (or standing still) is given by [1]

$$\overline{\Delta S}\left(\vec{r} \mapsto \vec{r}_j\right) = P_t\left(\vec{r}_j\right)[-S] + \left[1 - P_t\left(\vec{r}_j\right)\right] \sum_k \rho_k\left(\vec{r}_j\right) \Delta S_k \qquad k = 0, 1, 2, \ldots \tag{8}$$

The first term of the right hand side represents finding the source, it represents the chance of the source being at position $\vec{r}_j$ which would reduce entropy to zero, hence the $-S$ factor. This can be linked to exploitative behaviour, moving towards the position where the likelihood of finding the source is greatest. The second term corresponds to the case where the source is not found, but a number of hits can be detected. This represents exploratory behaviour, where the goal of the searcher is gaining more information, which comes in the form of hits.

The probability of k hits, denoted by $\rho_k(\vec{r}_j)$, during a time period Δt is

$$\rho_k = h^k e^{-h}/k! \tag{9}$$

as given by a Poisson law for independent detections. The expected number of hits h is estimated by

$$h(\vec{r}_j) \equiv \Delta t \int P_t(\vec{r}_0) R(\vec{r}_j|\vec{r}_0)\, d\vec{r}_0 \tag{10}$$

where $R(\vec{r}_j|\vec{r}_0)$ is the mean rate of encounters at position $\vec{r}_j$ with a source at position $\vec{r}_0$, as mentioned in the previous section (4).
The symbols ΔS_k in (8) denote the change in entropy between $P_{t+\Delta t}(\vec{r}_0)$ and $P_t(\vec{r}_0)$. First, $P_{t+\Delta t}(\vec{r}_j) = 0$ because the source has not been found. Secondly, the posterior probability distribution will be adjusted as a result of the k hits detected using (6).
The two terms on the right hand side of (8) show that infotaxis implements a balance between exploitative and exploratory behaviour.

3. Methods

3.1 Models of odour spreading

Two different models of odour spreading will be used. The first will be an irrotational potential flow [10] where the velocity field in the medium consists of two components, a flow in the positive y direction with the form $u = (ax + b)\hat{y}$ and a vortex that is compounded with a time-dependent modulation which takes the form $v = \frac{c}{r}\cos(\omega t)\hat{\theta}$. The total velocity field at position $\vec{x}$ at time t will then be given by

$$\vec{u}(\vec{x}, t) = (ax + b)\hat{y} + \frac{c}{r}\cos(\omega t)\hat{\theta} \tag{19}$$

where a, b, c and ω are constants. Variable r is the distance between the center of the vortex and $\vec{x}$, $\hat{y}$ is the unit vector in the positive y direction, and $\hat{\theta}$ is the unit vector perpendicular to the line between the center of the vortex and position $\vec{x}$. When the odour particle source is located near to the vortex center, the particle stream will be diffused by the flow, obscuring the exact location of the source from the view of the searcher.

The expected rate of encounters $R(\vec{r}|\vec{r}_0)$ as described in (4) will not be valid in this case. It will be shown that the width of the diffused plume caused by the vortex will not approach the $x \propto \sqrt{y}$ behaviour that would be expected [8]. In order to still have information on the expected rate of encounters, another preparation is made before the search process is started. Separately, a large number of particle releases are simulated. This simulation records the amount of particles passing through every lattice point. After normalization, this forms an estimate of the rate of encounters at a certain position relative to the source location.

The second model of the flow in the medium will be a simulation of a turbulent flow, advected by a mean wind in the positive y direction. The turbulent velocity field can be simulated by using kinematic simulation. The simulated field will present some of the important characteristics of a real turbulent flow, such as incompressibility and isotropy, in addition to adherence to a prescribed distribution over the available length scales. In this approach a velocity field is constructed by creating a sum of Fourier components.

$$\vec{u}(\vec{x}, t) = \sum_{n=1}^{N}\left[\vec{v}_n \cos\left(\vec{k}_n \cdot \vec{x} + \omega_n t\right) + \vec{w}_n \sin(\vec{k}_n \cdot \vec{x} + \omega_n t)\right]. \tag{11}$$

The wavenumbers $\vec{k}_n$ and the Fourier amplitudes $\vec{v}_n = \vec{v}(\vec{k}_n)$ and $\vec{w}_n = \vec{w}(\vec{k}_n)$ are chosen so that the velocity field $\vec{u}(\vec{x}, t)$ displays properties present in a realistic turbulent flow. The unsteadiness frequency ω_n is added to introduce a time dependence in this model. In this model the unsteadiness frequency of mode n is proportional to the eddy turnover time associated with wavevector $\vec{k}_n$ as [7]

$$\omega_n = \lambda\sqrt{k_n^3\, E(k_n)}, \tag{12}$$

where λ is an adjustable weighting factor and $E(k)$ is the Kolmogorov spectrum in the inertial range [9].

In order for the velocity field to be incompressible, the field needs to comply with $\nabla \cdot \vec{u} = 0$. This means that

$$v_{x,n}k_{x,n}\ \cos\left(\vec{k}_n \cdot \vec{x} + \omega_n t\right) + w_{x,n}k_{x,n}\sin\left(\vec{k}_n \cdot \vec{x} + \omega_n t\right) + v_{y,n}k_{y,n}\ \cos\left(\vec{k}_n \cdot \vec{x} + \omega_n t\right) + w_{y,n}k_{y,n}\sin\left(\vec{k}_n \cdot \vec{x} + \omega_n t\right) = 0\ . \quad (13)$$

This is equivalent to

$$\left(\vec{v}_n \cdot \vec{k}_n\right)\ \cos\left(\vec{k}_n \cdot \vec{x} + \omega_n t\right) + \left(\vec{w}_n \cdot \vec{k}_n\right)\sin\left(\vec{k}_n \cdot \vec{x} + \omega_n t\right) = 0. \quad (14)$$

This can be achieved by choosing Fourier amplitudes so that $\left(\vec{v}_n \cdot \vec{k}_n\right) = \left(\vec{w}_n \cdot \vec{k}_n\right) = 0$, i.e. choosing $\vec{v}_n$ and $\vec{w}_n$ perpendicular to $\vec{k}_n$.

The vectors $\vec{k}_n$, $\vec{v}_n$ and $\vec{w}_n$ will be chosen in a way that simulates a flow that is in accordance with the aforementioned Kolmogorov spectrum [9]:

$$E(k) = C\epsilon^{2/3}k^{-5/3}, \quad (15)$$

where the Kolmogorov constant C is taken to be 1.5 . The wavenumbers k_n will be a discretized segment of the wavenumber space between the small scale cutoff $k_\eta = 2\pi/\eta$ and integral scale $k_c = 2\pi/L$, which represents the largest contributing length scale in the flow. The Kolmogorov length η [9], the smallest relevant length scale, is given by

$$\eta = \left(\frac{v^3}{\epsilon}\right)^{\frac{1}{4}}, \quad (16)$$

with kinematic viscosity v and turbulent dissipation per unit mass ϵ. The energy is set to zero for $k < k_c$ and $k > k_\eta$. In 2D, the N_k vectors $\vec{k}_n$ are taken from a circle of radius k_n, with random direction. The wavenumbers k_n are geometrically distributed over the range of k_c to k_η.

$$k_n = k_c\left(\frac{k_\eta}{k_c}\right)^{n-1/N_k-1} \qquad n = 1 \ldots N_k. \quad (17)$$

As mentioned before, the directions of the vectors $\vec{v}_n$ and $\vec{w}_n$ are chosen perpendicular to $\vec{k}_n$. In order to make sure each mode represents a part of the energy spectrum, their lengths are taken from the energy shells $E(k_n)$ as [7]

$$\frac{1}{2}v_n^2 = \frac{1}{2}w_n^2 = E(k_n)\Delta k_n \quad (18)$$

with

$$\Delta k_n = \frac{k_{n-1}+k_{n+1}}{2}.$$

In both cases, the velocity field $\vec{u}(\vec{x}, t)$ generated by the model is used to integrate $\frac{d\vec{x}}{dt} = \vec{u}(\vec{x}, t)$ using a 4th order Runge-Kutta scheme to calculate the movement of the odour particles.

3.2 Infotaxis

Using the theory behind infotaxis given in the previous chapter, a short step by step search algorithm will be given in this section. This approach is the same for all different models of odour spreading, only the expected rate of encounters $R(\vec{r}|\vec{r}_0)$ will vary.

Beforehand, an initial configuration of the posterior distribution for the location of the source $P_0(\vec{r}_0)$ must be chosen. In this case, the searcher detects a hit at $t = 0$, which according to (5) results in $P_0(\vec{r}_0) = R(\vec{r}(t = 0)|\vec{r}_0)/Z$, where Z is a normalizing constant. In order to achieve this situation, particles are simulated prior to the searcher starting its movement process, using the relevant flow model as described in section 3.1. When a particle collides with the searcher, the probability distribution is known and the searcher starts moving. As an added bonus, this makes sure there are already several particles spread out in the medium at the start of the searching process.

Now, the actual searching algorithm begins, with the searcher waiting for a length of time δt. During this time, the movement of the odour particles is simulated and the number of particle detections is recorded. After this period, the probability distribution for the source location $P_t(\vec{r}_0)$ is updated with regard to the number of hits during time interval δt, using (6). This new probability distribution can then be used to calculate the current Shannon's entropy S from (7). Then, for the four neighbouring points and the searcher's own position, the expected reduction in entropy $\overline{\Delta S}$ is calculated using (8). The position where $\overline{\Delta S}$ is most negative is chosen as the new position for the searcher. This process is repeated until the searcher reaches the source location, hits the edge of the search window or when the search goes on for too many timesteps.

4. Results and discussion

4.1 Chaotic advection

First, the effectiveness of the odour spreading model involving a vortex is investigated. The goal of this model is to create a state of deterministic chaos. Even though the field is fully deterministic, a small change in starting position of a particle can result in a large change in the movement path of said particle. The movement of a small number of particles has been simulated in Figure 1.

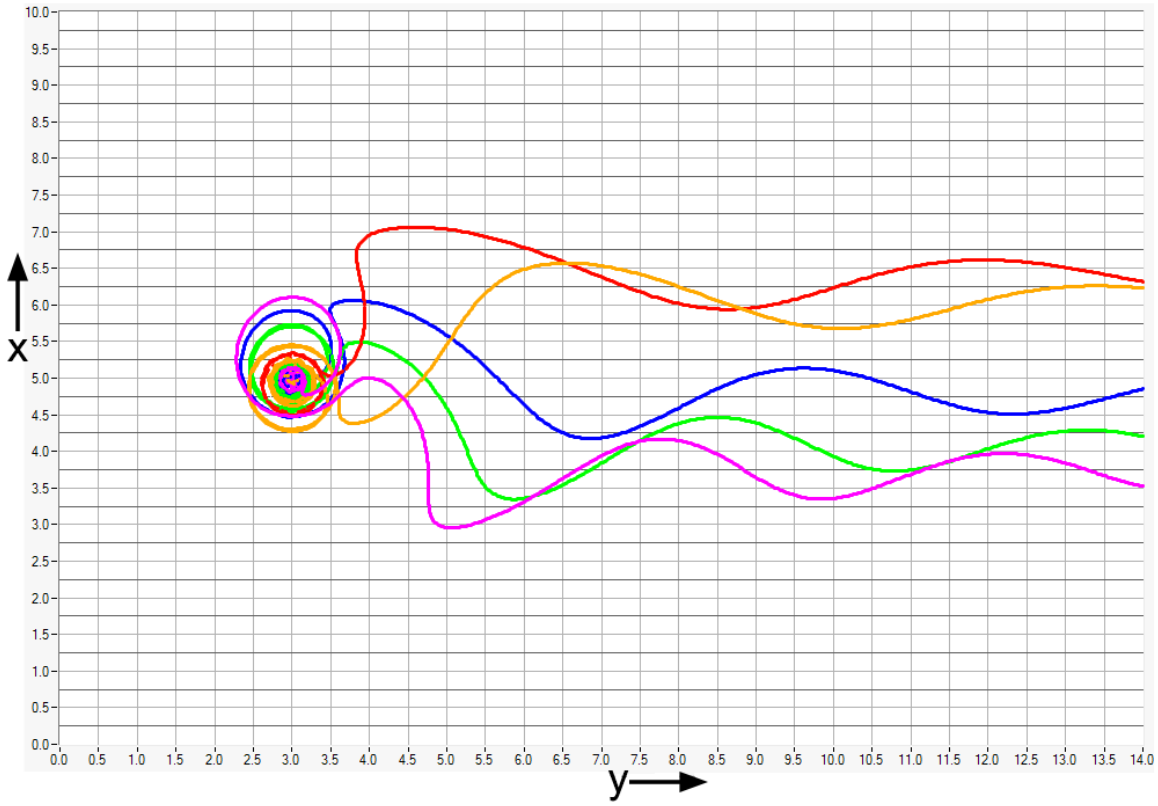

Figure 1: Simulation of five particle movement paths in a velocity field described by (19). At $t = 0$, all particles are located on the line $x = 5$. The distance between the starting positions of the particles is 0.1

The image shows that the model works as intended. A change in starting position of 0.1 results in a drastic change of the distance from the central line $x = 5$, up to forty times the initial adjustment. Figure 1 also gives reason to suspect this velocity field may only diffuse particles near the vortex location, after which they move in positive y-direction with only slight oscillation in the x-direction.

As stated in section 3.1, it is necessary to gather information on the expected rate of encounters $R(\vec{r}|\vec{r}_0)$ before an actual search can be started. Simulating a large number of particles being advected by the described velocity field has yielded the data illustrated in Figure 2.

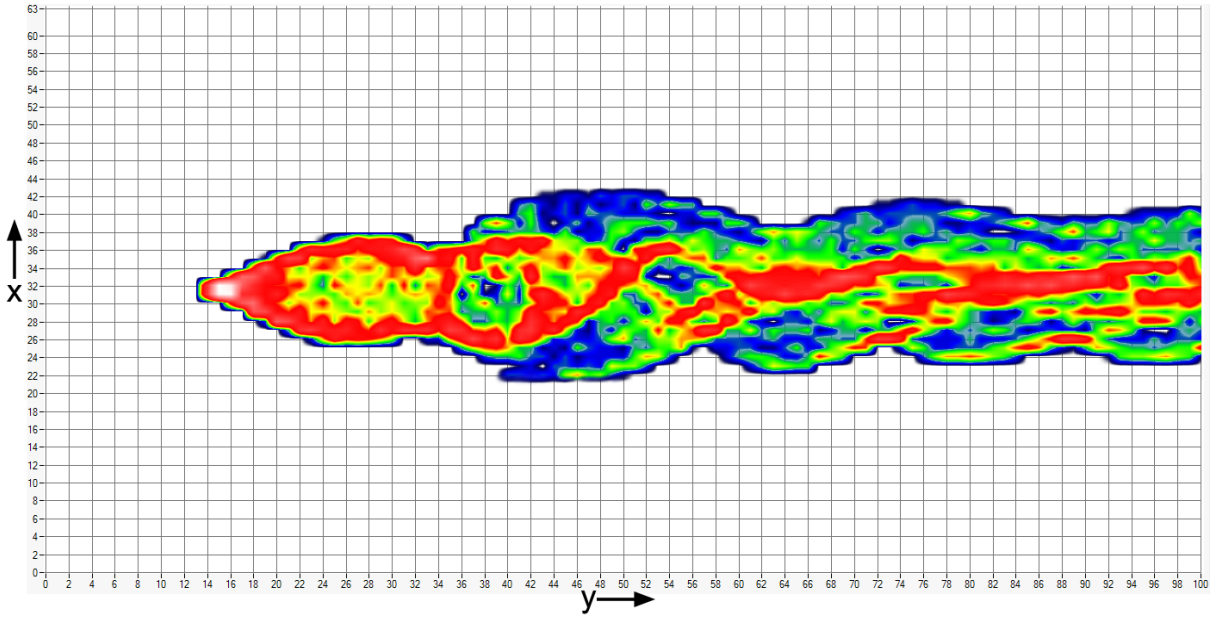

Figure 2: Simulation of the expected rate of encounters at a lattice point. In this image, the white patch on the left side of the plume indicates the highest rate of encounters, followed by red, yellow, green and blue. The odour source is located at $(\mathrm{x},\mathrm{y}) = (32{,}15)$ and the center of the vortex is located at position $(32{,}39)$.

This graph shows strong similarities to the paths observed in Figure 1, as expected. The vortex spreads the odour plume out over a wider area, after which the particles only seem to oscillate slightly. It is clear that the width of this plume does not behave like $x \propto \sqrt{y}$ for higher values of y. This justifies the use of this pre-simulated approach for the expected rate of encounters, since the values calculated from (4) will not be accurate for this velocity field. When the searcher is for example positioned at position $(x, y) = (10{,}80)$ in Figure 2, an estimate for the odour plume using (4) would yield a non-zero value for the rate of encounters. As can be seen from the image above, the real plume has a sharply bounded and near constant width at those values for y, and the actual expected rate of encounters is zero.

Using the information that has been gathered on the expected rate of encounters, the infotaxis algorithm can be applied. An example of the path followed by the searcher during one run of the process is shown in Figure 3.

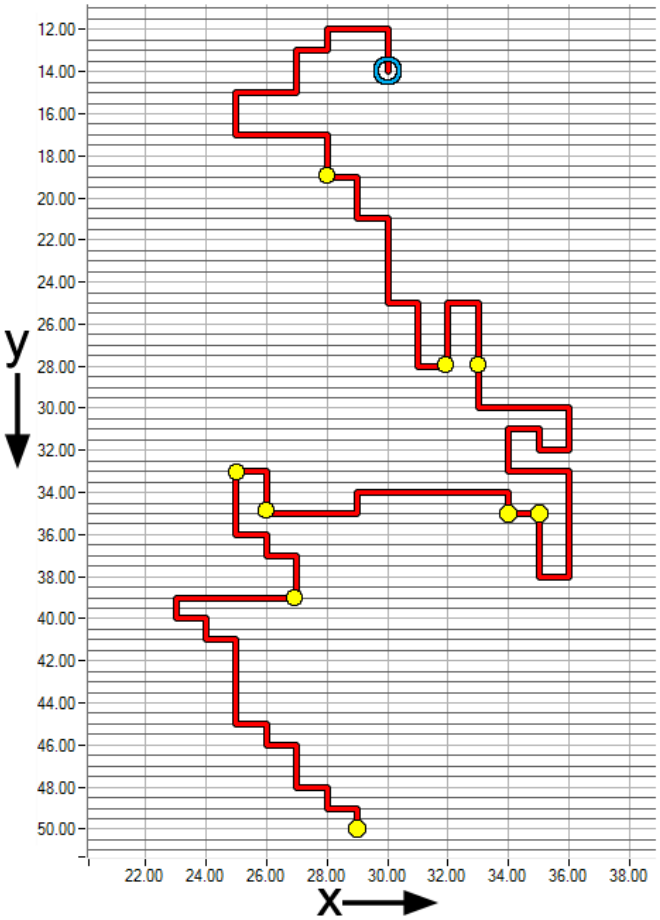

Figure 3: Illustration of the path (marked as red) travelled by the searcher on a successful run of the infotaxis algorithm. The position of the odour source is marked with a blue ring. Odour encounters are marked as yellow circles. The searcher starts at position $(\mathrm{x}, \mathrm{y}) = (29,50)$ and starts moving when the first hit is detected.

This image shows that when using the strategy of infotaxis, odour encounters can have a strong influence on the movement of the searcher. As expected from (6), a hit can have a large effect on the probability distribution for the location of the source. Near to position $(x, y) = (35,26)$, two odour encounters cause the searcher to turn from a movement predominantly in the negative y-direction towards the positive x-direction. This then occurs in reverse when two more hits are recorded near $(x, y) = (35,35)$. In this case, the rate of detected encounters does not increase greatly during the last steps near the source, as would be expected. This can however be explained by the fact that the last steps of the searcher are done at the 'sides' and 'bottom' of the source, where particles are not likely to travel (as seen in Figure 2).

Now, some statistics of the infotaxis algorithm will be evaluated. The algorithm was run on a number of different velocity fields, created by varying the flow parameters a, b, c and ω in (19). The success rate of the search process was affected by the accuracy of $R(\vec{r}|\vec{r}_0)$, as can be expected. With the odour spreading flow parameters at the exact values used in calculating $R(\vec{r}|\vec{r}_0)$, the success rate of the searcher was 82%. Varying the parameters of the actual flow with a random factor of $\pm 20\%$ of the parameter value reduced the success rate to 55%. A significant reason for this reduction in success could have been the estimated plume width not coinciding with the actual plume width. If the plume would be expected to be wider than it actually was, it could cause the expected rate of encounters to be high at a position too far to the side, where no detections are possible. This means that the searcher would expect to gain information at positions at too high or too low values for x, increasing the chances of hitting the edges at the sides. It could also cause the searcher to expect the plume to be very narrow, leading to it only exploring a narrow corridor in the medium, moving past the source and hitting the edge at $y = 0$.

In order to investigate the behaviour of the duration of the search process, the average search time has been plotted against the initial distance between the source and searcher in Figure 4.

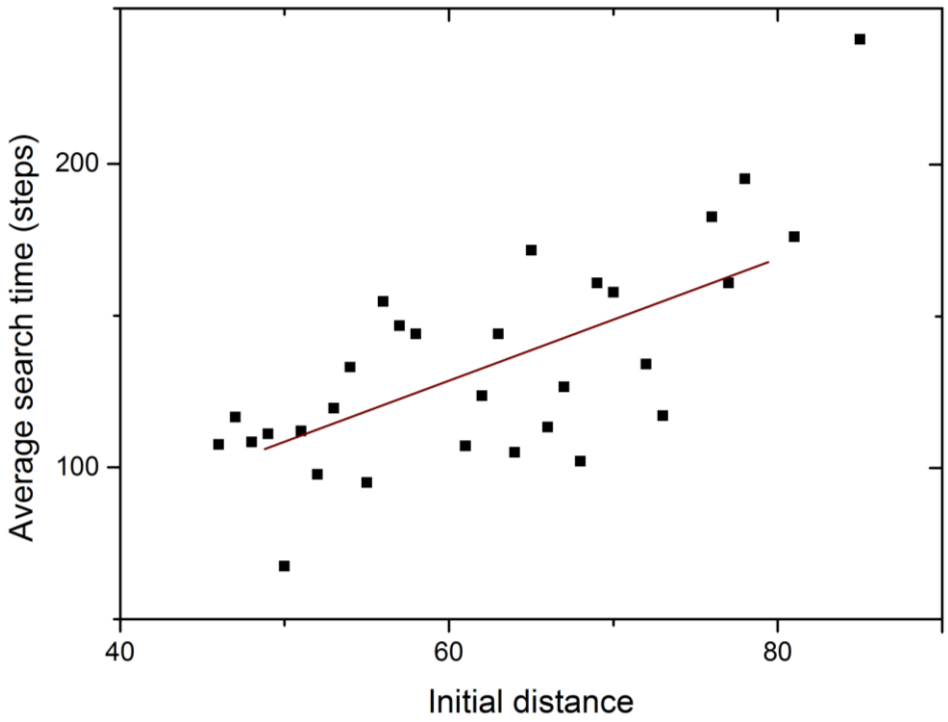

Figure 4: The average search time (in number of steps) plotted against the initial distance between the source and searcher. The search time has been averaged across four search runs. A line has been fitted through these data points, given by $T = 7.9 + 2.0r$, with T the average search time, and r the initial distance.

The graph shows that the search time increases with the initial distance, as expected. The data points however do not seem grouped enough to merit a strong claim on the details of this behaviour. The average search time increasing with $T \propto r$ seems possible, but it is not the only viable option here. In order to definitively confirm or disprove this relation between the search time and initial distance, the algorithm could be run with larger variance in initial distances. The search time could also be averaged over a larger number of search paths.

Finally, the link between information and search time has been evaluated by plotting the entropy of the probability distribution for the source location against the search time, as shown in Figure 5.

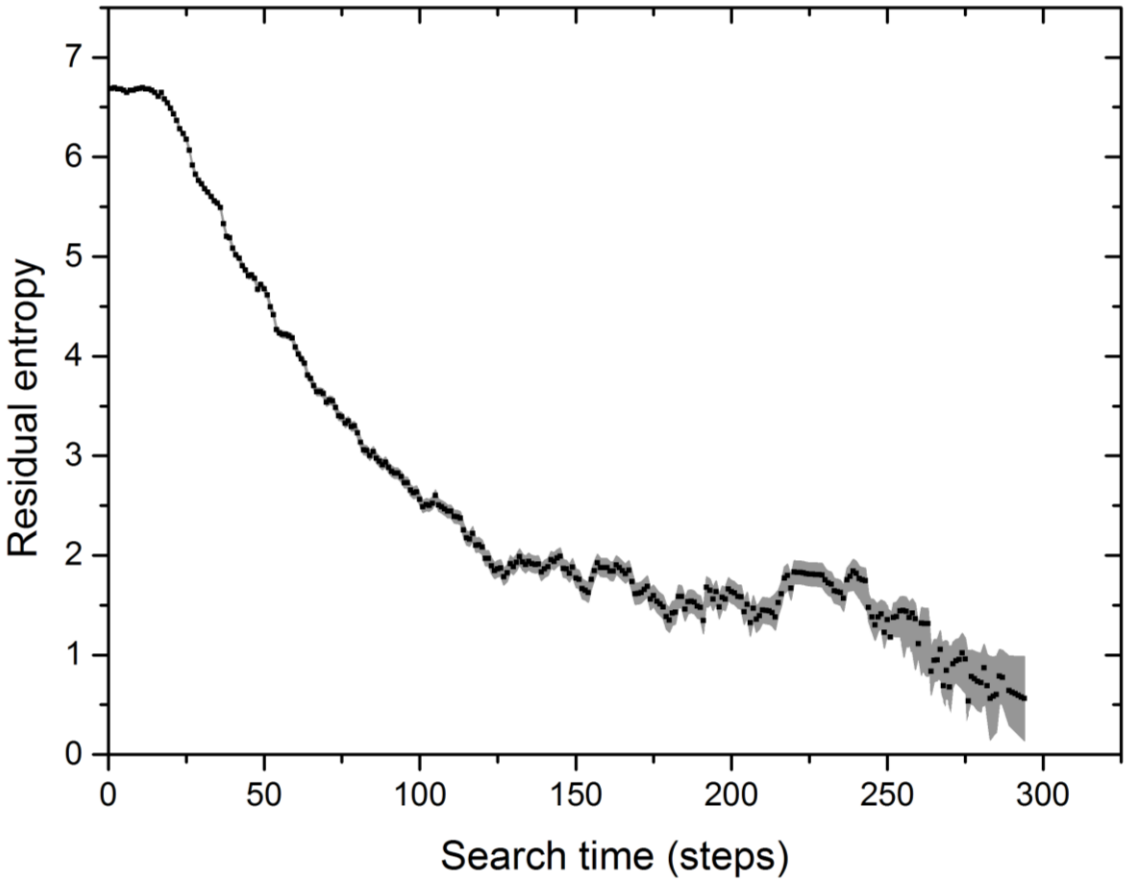

Figure 5: The average residual entropy of $P_t(\vec{r}_0)$ plotted against the search time (in number of steps). The entropy has been averaged across 70 search runs. The standard deviation in the entropy is shown as a grey area.

Following this graph, at first the average residual entropy does not change a significant amount. This is explained by the fact that the searcher has not experienced many odour encounters yet. The searcher will move more randomly at first, moving in a more defined direction when multiple hits have been detected. Once a clear direction arises, the entropy will continue a net decrease. It will only increase for a short period of time when the searcher 'takes a wrong turn' and gets stuck in an area of little benefit. It will then move out of this area by taking a route which increases the entropy the smallest amount.

In the data used for Figure 5, successful search runs ended anywhere between 110 and 300 steps. Near the end of a search, the entropy of the probability distribution for the source location has not reached $S = 0$. This is caused by the fact that the source location is unknown until the searcher reaches said location. The probability distribution will most likely be narrowed down to a smaller area, but there will still be uncertainty. This means there is information left to gain, which in turn means there is still residual entropy.

4.2 Kinematic simulation

Now, the infotaxis algorithm is applied to a flow constructed with kinematic simulation, as described in section 3.1. First, the expected rate of encounters $R(\vec{r}|\vec{r}_0)$ at position $\vec{r}$ for a source at position $\vec{r}_0$ is estimated in the same way as was done in the previous model in order to get a visualization of the flow. This estimation is illustrated in Figure 6.

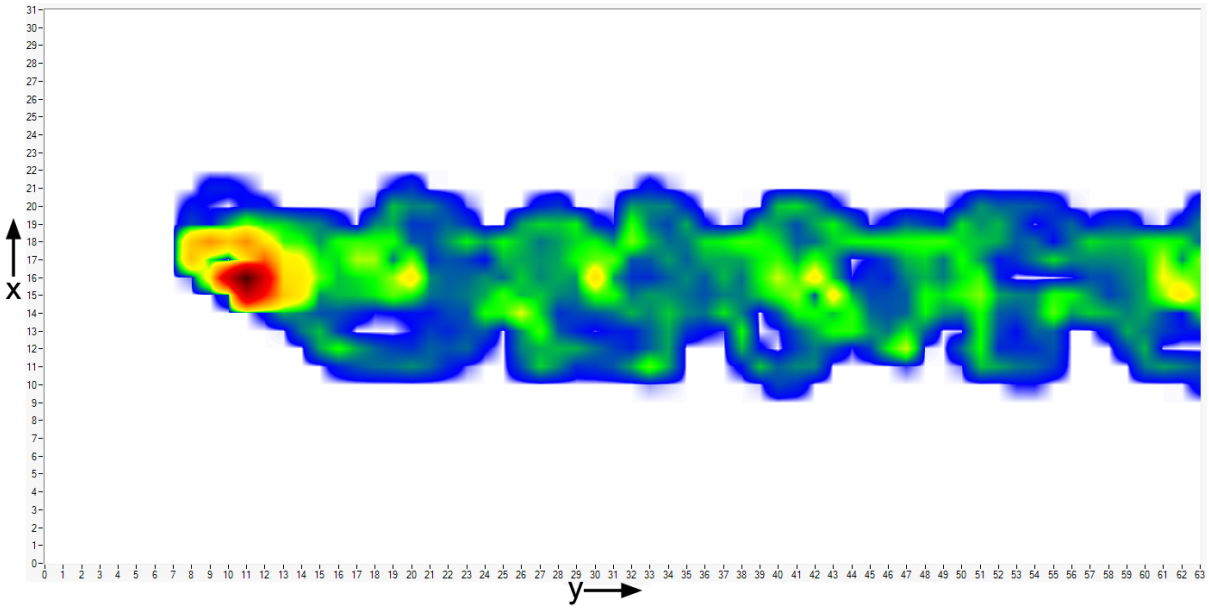

Figure 6: Visualization of the flow constructed using kinematic simulation. This image was constructed using 100 particles, with $N_k = 20$ modes in the kinematic simulation. The black spot indicates the highest expected rate of encounters around the source location at $(x, y) = (16,12)$. The lower magnitudes are shown in red, followed by yellow, green and blue.

The plume created by this odour spreading model appears narrower than expected at higher values for y. As mentioned in section 3.1, in a real turbulent flow the width of the plume would approximately follow $x \propto \sqrt{y}$. The image also shows clearly identifiable particle paths in the plume. This means that the flow was not sufficiently chaotic to realistically represent a true turbulent flow. Spreading out the individual particle paths more would possibly involve increasing the amount of modes N_k in the kinematic simulation. This would however increase all simulation times greatly, since the time needed for a single particle movement timestep of the kinematic simulation increases with $O(N_k)$. The choice has been made to use the approximation for the expected rate of encounters as described in (4) regardless, in order to test its effectiveness in non-optimal conditions.

The infotaxis algorithm can now be applied on the flow created with kinematic simulation. Instead of relying on the premade estimation of the expected rate of encounters $R(\vec{r}|\vec{r}_0)$ from Figure 6, the approximation for $R(\vec{r}|\vec{r}_0)$ as given in (4) is used. An example of the path travelled by a searcher applying the strategy of infotaxis is shown in Figure 7.

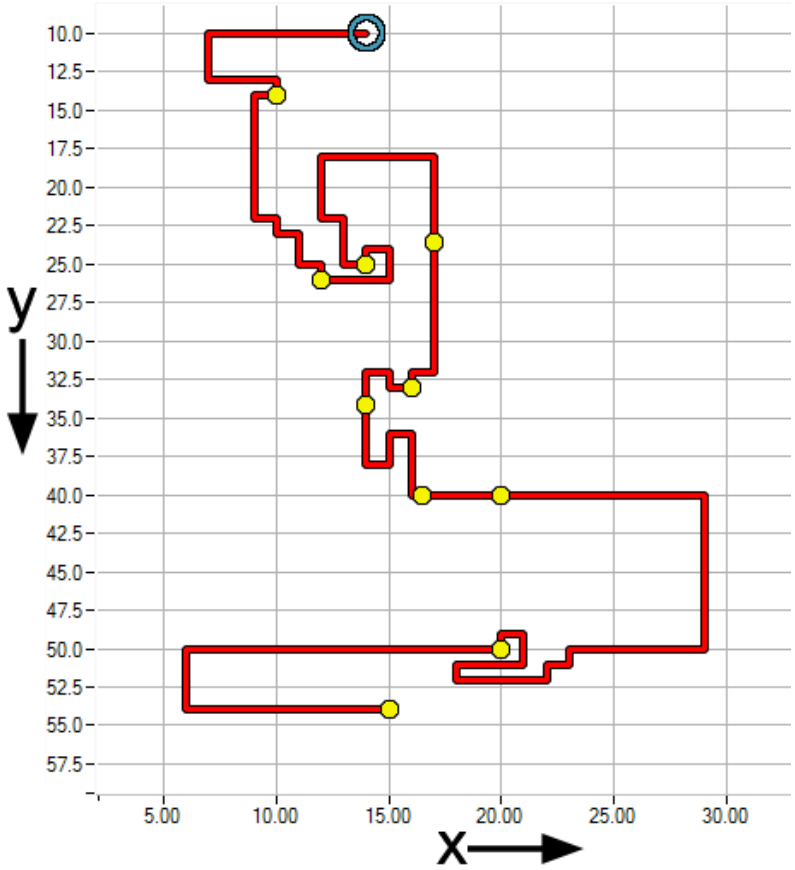

Figure 7: Illustration of the path (marked as red) travelled by the searcher on a successful run of the infotaxis algorithm. The position of the odour source is marked with a blue circle. Odour encounters are marked as yellow circles. The searcher starts at position $(x, y) = (15{,}54)$ and starts moving when the first hit is detected.

The image gives an indication of the behaviour of infotaxis in both the absence and presence of hits. When no hits are detected, the searcher shows large left to right casting paths, exploring a large area. In the event of an odour encounter, the searcher often starts doing a high density zigzag. As can be seen in (6), a hit increases the probability of the source being close to the location of the searcher at that time. This causes the searcher to explore its immediate surroundings when an odour encounter is recorded. If no hits are detected during a period of close-range exploration afterwards, the probability distribution will decrease again near the searcher, triggering a more long-range exploration. This can be observed in Figure 7 around the hit at $(x, y) = (20{,}50)$.

Next, some statistics will be evaluated for the infotaxis algorithm when applied to the flow constructed by kinematic simulation. The success rate of the search process was at around 60%. This is lower than the success rate for the chaotic advection flow, but this is to be expected from the implementation of the expected rate of encounters. In the previous section, a precalculated rate of encounters was used. This meant that the expected rate of encounters was near perfect, where the expected rate of encounters here was an approximation, as mentioned in chapter 2.
The success rate of the infotaxis strategy in the case where the flow parameters of the chaotic advection were semi-randomized, causing the expected rate of encounters to be an approximation as well, was closer to the success rate here (55%).

In order to further compare the infotaxis algorithm in these two cases, the average search time has been plotted against the initial distance between the source and searcher in Figure 9.

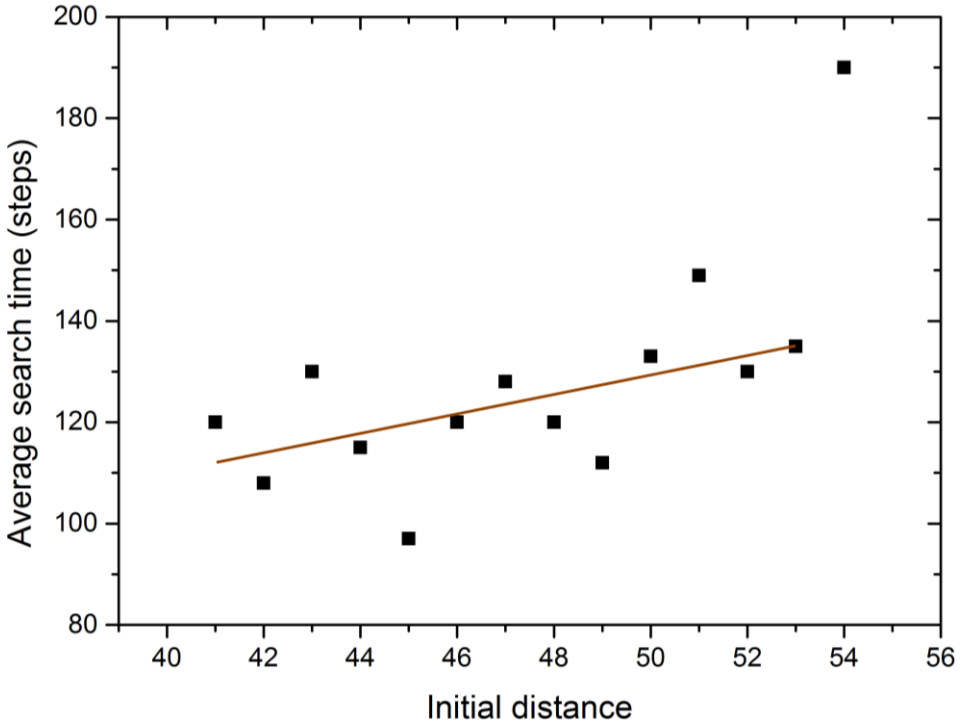

Figure 8: The average search time (in number of steps) plotted against the initial distance between the source and searcher. The search time has been averaged across three search runs. A line has been fitted through these data points, given by $T = 38.0 + 1.8r$, with T the average search time, and $\boldsymbol{r}$ the initial distance.

Again, the graph shows that the search time increases with the initial distance, as expected. Comparing this to the previous odour spreading model, the slope of this graph is close to the slope in Figure 4. This is an indication that infotaxis is consistent across different types of flows. However, the average search time in the kinematic simulation model is about 25 steps higher than that in the chaotic advection model for any given initial distance. This indicates that infotaxis is slightly less effective in this situation, further strengthening the point mentioned earlier that the use of an approximation of the expected rate of encounters lessens the performance of the algorithm.

As a final comparison between the two odour spreading models, the link between information and search time has been evaluated by plotting the entropy of the probability distribution for the source location $P_t(\vec{r}_0)$ against the search time, as shown in Figure 9.

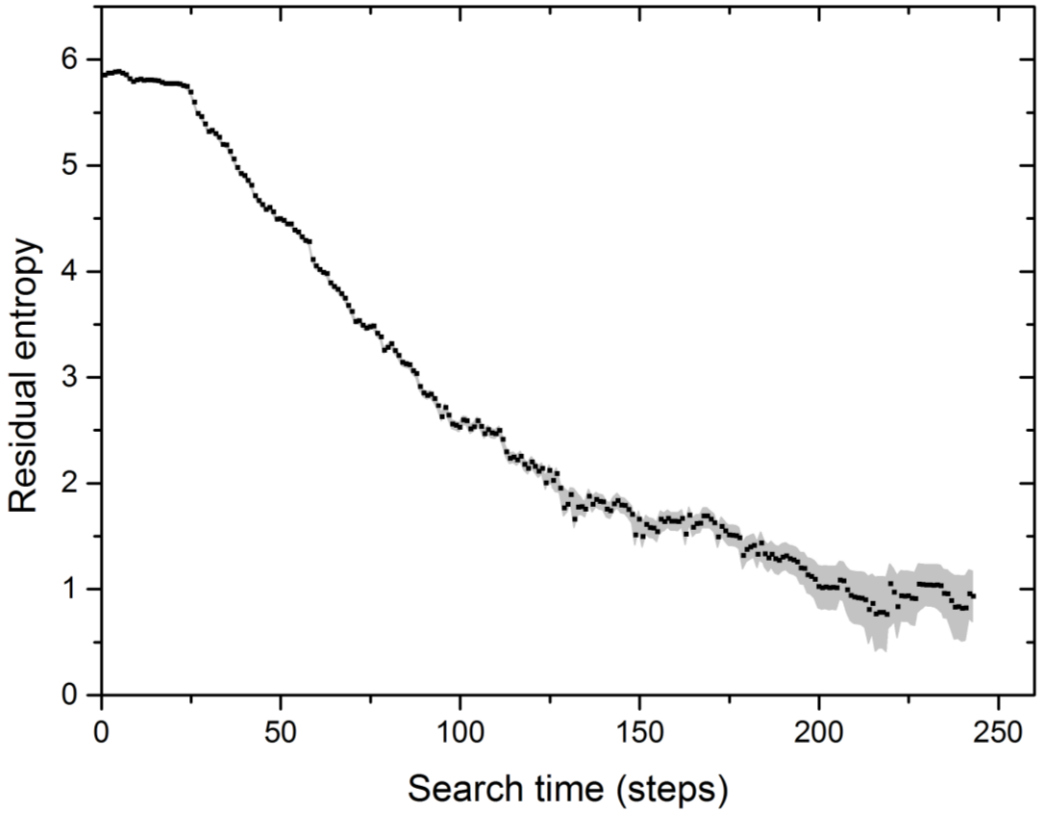

Figure 9: The average residual entropy of $P_t(\vec{r}_0)$ plotted against the search time passed (in number of steps). The entropy has been averaged across 40 search runs. The standard deviation in the entropy is shown as a grey area.

This graph is very similar to that of the chaotic advection flow, as shown in Figure 5. The entropy does not show a strong decrease at the start of the search, because the movement of the searcher is near random at first, since there have been almost no odour detections recorded yet. The entropy at the end of the search is not zero, because the source location does not need to be pinpointed exactly before it can be found.

The entropy starts at a lower value than the average entropy in the previous model as shown in Figure 5. This is caused by the fact that the grid on which these searches took place was chosen to have a smaller amount of grid squares, to counteract longer search times caused by the kinematic simulation calculations.

In Figure 10, an example of a short successful search path is compared to an example of a longer search path.

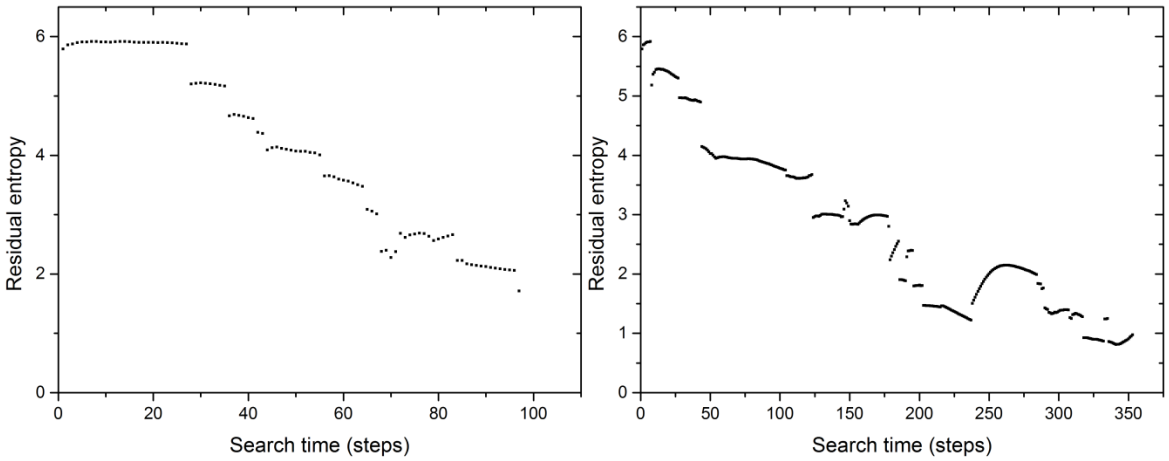

Figure 10: The residual entropy of $P_t(\vec{r}_0)$ plotted against the search time (in number of steps) during two successful search paths. The image on the left shows a shorter path, the image on the right shows a longer path. The jumps in entropy are caused by the change in probability distribution due to odour detections.

This image, containing two characteristic search paths, shows that a dip in entropy can appear in the longer search paths. The reason the searcher in the graph on the right takes longer to get to the source, is the fact that it gets stuck in an 'entropy well'. In such a situation, a high frequency of odour detections in a short time period has caused the probability distribution for the source to be sharply defined near the searcher, but not near the actual location of the source. Because the probability distribution is sharply defined, the entropy will be low. This means the searcher does not expect to gain anything from moving far away from this location. It will take time or new odour detections to coax the searcher into moving in a direction which increases entropy, in order to get out of this well.

In the image on the right, the searcher records a high amount of hits in between 175 and 200 steps remaining. This causes the entropy to be low, which constrains the searcher until 120 steps remaining, where a new odour encounter triggers the recovery from the entropy well. These types of entropy wells appear with greater frequency in this model than in the model of chaotic advection. This could contribute to why the average search time is higher in this model than in the model of chaotic advection, for the same initial distance. It is unclear whether this vulnerability to entropy wells is due to the odour spreading model or the approximation for $R(\vec{r}|\vec{r}_0)$ as given by (4). It is possibly caused by the combination of the two. As seen in Figure 6, there are slight hotspots of expected encounter rate in this flow. These do not exist in the particle dispersion model described in (4). This means that when a searcher records a high frequency of hits in one of these hotspots, the description of $R(\vec{r}|\vec{r}_0)$ does not account for the fact that the source may still be far away, leading the probability distribution to be too sharply localized near the searcher.

The image on the right also shows that a longer search path often leads to lower residual entropy when the source is found. This is caused by a higher total number of hits, due to the fact that the searcher has spent more time inside the flow, as well as a higher amount of explored locations. The searcher has visited a larger number of grid points, which did not contain the source, causing them not to contribute to the probability distribution anymore. This helps defining the source location more sharply, reducing the total residual entropy.

5. Conclusion

The search strategy of Infotaxis has been shown to be effective at locating the source of an odour trace in a flowing medium. Movement of a searcher based on infotaxis shows large casting paths and short range zigzagging. When no hits are detected, the searcher shows large left to right casting paths, exploring a large area. In the event of an odour encounter, the searcher often starts doing a high density zigzag, exploring a tight area.

Infotaxis has been shown to be effective in two different types of odour spreading flow, chaotic advection and an approximation of a turbulent flow constructed by kinematic simulation. In both cases, the search time increased linearly with (sufficiently high) initial distance from the source. Due to the shape of the odour plume close to the source, the average search time is higher in the kinematic simulation flow. In both models, the uncertainty in the information, represented by the entropy in the probability distribution for the location of the source, is generally consistently reduced during the search process. However, the searcher is more vulnerable to getting stuck in an entropy well in the kinematic simulation model. Due to the fact that the source location is not necessarily known before the source is encountered, the source is found with non-zero entropy remaining.

This investigation could be expanded upon in multiple ways. The most obvious one is carrying out the simulations for longer periods of time. This could include increasing the amount of modes in the kinematic simulation in order to make that a more realistic representation of a turbulent flow. Executing more search runs would help strengthen conclusions about the behaviour of the average search time in relation to the initial distance, as well as average out anomalies in the residual entropy in relation to the residual search time caused by less successful search paths. Enlarging the grid size on which the search takes place would allow for higher initial distances and longer search paths, further helping the search time and entropy examinations.

Since the effectiveness of infotaxis in two different situations has been shown, another way to expand on this investigation would be to attempt to apply the strategy in different situations. An interesting case would of course be to not use a flow approximation like in this investigation, but to use a solution of the Navier-Stokes equation to calculate movement of odour particles. Further investigation could also involve designing a variant of infotaxis that involves continuous movement of the searcher instead of a grid-based system. Another idea would be to use multiple searchers simultaneously, sharing the information they acquire. Finally, infotaxis could be applied in a situation involving searching based on sparse information, but not involving any fluid flow to spread the signal.

6. References

1. Vergassola, M., Villermaux, E., Shraiman, B.I., *'Infotaxis' as a strategy for searching without gradients*. Nature **445**, 406-409 (2007)
2. Kennedy, J.S. *Zigzagging and casting as a preprogrammed response to windborne odour: A review.* Physiol. Entomol. **27**, 58-66 (1983)
3. Russel, R. A. *Odor Detection by Mobile Robots*, World Scientific, Singapore, (1999)
4. Smoluchowski, M.V. *Versuch einer mathematischen theorie des koagulationslinetic kolloider Lösungen*. Z. Phys. Chem. **92**, 129-168 (1917)
5. Masson, J-B, Bailly Bechet, M. and Vergassola, M. *Chasing information to search in random environments*. J. Phys. A: Math. Theor. **42** (2009)
6. Shannon, C.E. *A Mathematical Theory of Communication*. Bell Sys. Tech. Journ. **27**, 379-423, 623-656, (1948)
7. Elenbaas, T. *Writing lines in turbulent air using Air Photolysis And Recombination Tracking*. PhD thesis, Technische Universiteit Eindhoven, Eindhoven, (2005)
8. Taylor, G.I. Proc. London Mathematical Society **20**, 196-211, (1921).
9. Pope, S.B. *Turbulent flows, Cambridge University Press*, Cambridge, (2000)
10. Kunda, P.K. and Cohen, I.M. *Fluid Mechanics (2nd ed.),* Academic Press, San Diego, (2002)